

# DESIGN AND IMPLEMENTATION OF SNS RING VACUUM SYSTEM WITH SUPPRESSION OF ELECTRON CLOUD INSTABILITY\*

H. Hseuh<sup>1</sup>, M. Blaskiewicz, P. He, M. Mapes, R. Todd, L. Wang, J. Wei, S.Y. Zhang, BNL, USA

## Abstract

The Spallation Neutron Source (SNS) ring is designed to accumulate, via  $H^-$  injection,  $1.6 \times 10^{14}$  protons per pulse at 60 Hz and 1 GeV energy [1]. At such beam intensity, electron cloud is expected to be one of the intensity-limiting mechanisms that will complicate ring operation. This paper presents the design of the ring vacuum system and the mitigation strategy adopted to suppress the electron cloud instability. These measures include the titanium nitride (TiN) coating of the chamber walls to reduce the secondary electron yield (SEY), the tapered magnetic field for the collection of the stripped electrons at injection, clearing electrode dedicated for the injection region and parasitic ones using the BPMs around the ring, solenoid windings in the field free regions, and the possibility of beam scrubbing at high pressure.

## SNS RING VACUUM SYSTEM

The SNS ring, with a four-fold symmetry and a circumference of 248 m, consists of 4 arc sections of 34 m each with FODO lattice and 4 straight sections of 28 m each with doublet lattice [1]. Each ring arc section has 8 halfcells and one quartercell. The halfcell magnets and vacuum chambers [2] are symmetrically grouped to the middle quartercell, such that they are mirror images to each other with respect to the center quartercell. This strategy reduces the individual chamber components into two types, lowering the cost of fabrication and assembly. Each halfcell chamber, as shown in Fig. 1, consists of a dipole chamber section, pump ports, quadrupole section, BPM and bellows. The 2 m long dipole chamber has a very large elliptical cross section of 23 cm (H) x 17 cm (V), curved with a bending angle of  $11.25^\circ$ . The halfcell chambers are  $\sim 4$  m long and made of stainless steel 316L or 316LN. To avoid radiation induced stress corrosion, the bellows are fabricated with inconel 625. In all, there are four types of halfcell chambers; three with 21 cm quadrupole pipe and one with 26 cm quadrupole pipe.

\* SNS is managed by UT-Battelle, LLC, under contract DE-AC05-00OR22725 for the U.S. Department of Energy. SNS is a partnership of six national laboratories: Argonne, Brookhaven, Jefferson, Lawrence Berkeley, Los Alamos, and Oak Ridge.

<sup>1</sup>Corresponding author email: hseuh@bnl.gov .

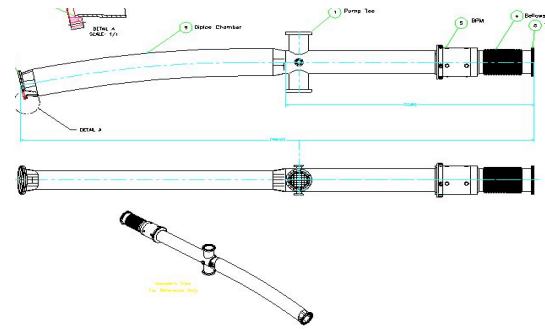


Fig.1 Schematics of SNS ring arc halfcell chambers. Each chamber is  $\sim 4$  m long and fabricated with 316L stainless steel and inconel bellows.

The four straight sections are dedicated for injection, collimation, extraction, and RF and diagnostics. Each straight section has two sets of doublet magnets. The two doublet chambers in each section are identical, except at the extraction section, which reduces the number of spares for the future. Each doublet chamber consists of a 30 cm OD straight pipe welded to the 30cm bellows and BPM. The length of the doublet chambers ranges from 3 m to 5 m, as shown in Fig. 2. The balance of the straight sections is occupied by special chambers housing the injection, collimation, rf, extraction and diagnostic equipment.

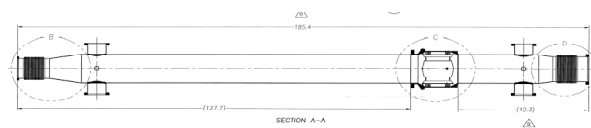


Fig. 2. Schematics of typical SNS ring straight section doublet chambers for 30 cm quadrupole doublets.

The electron-cloud effect in the SNS ring is expected to be one of the intensity-limiting mechanisms and a potential threat to the high-intensity operations [3]. Main sources of electrons are: electrons generated at the injection stripping foil, from proton grazing losses at the collimator surface and other chamber wall, beam induced multipacting, and from beam residual gas ionization. The electron-cloud effects include neutralization tune shift and resonance crossing, electron-cloud instability, emittance growth and beam loss, pressure increase, heating of the vacuum pipe and interference with beam diagnostics. To combat the electron-cloud effects, several measures have been adopted

at the design stage of the vacuum systems and implemented. Detailed description of these measures is given in the following sections.

### TITANIUM NITRIDE COATING

One major contributing factor to the electron multipacting is the secondary electron emission (SEY) of the vacuum surface facing the beam. Most SNS ring chambers are fabricated from stainless steel, which has a peak SEY of  $\sim 2.5$ . The SEY can be reduced to  $< 2$  if the surface is coated with titanium nitride (TiN) [4]. TiN coating has been routinely applied to high power RF windows and tuners to reduce multipacting. TiN coating of regular accelerator beam tubes was done for PEP-II LER [5] using DC sputtering. Due to the large cross sections of the SNS chambers, magnetron DC (MDC) sputtering was developed for TiN coating for its high deposition rate, low operating voltage and pressure [6]. This is a result of the increased plasma density formed by the electrons confined within the magnetic field, which adds to the sputtering rate. Improved stoichiometry and uniformity were also achieved with MDC. NEG coating was considered but not adopted since the ring vacuum system is not designed for *in-situ* bake, which is needed to activate NEG and achieve low SEY for the coated surface. *In-situ* bake of the SNS ring vacuum system posts high risk to the large aperture flanges which tend to leak due to relative thermal motion. Reliability of the bakeout systems over long period of time in a high radiation environment is also not proven.

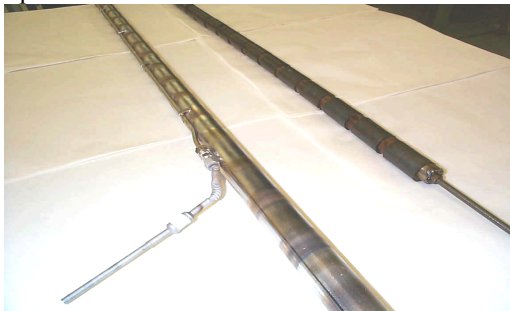


Fig. 3 A long titanium cathode for magnetron DC sputtering of TiN coating for SNS vacuum chambers. The permanent magnets/spacers enhance the discharge plasma density thus the deposition rate.

Much work has been done on the formation of TiN by magnetron sputtering as an industrial hard coating using planar electrodes and magnets. Due to the SNS chamber geometry, a linear titanium cathode with a suitable magnetic field was developed as shown in Fig. 3. Commercially available *Alnico* magnets are inserted in a 1.5" diameter titanium tube used as a cathode. The magnets are stacked with 0.5" spacers resulting in a looping magnetic field of several hundred gauss projected from the cathode surface. The 0.5" diameter hole in the center of the magnets allows for water cooling of the cathode. This "low cost" cathode works

in conjunction with a 10 KW DC power supply to produce a satisfactory field and discharge plasma as shown in Fig. 4.

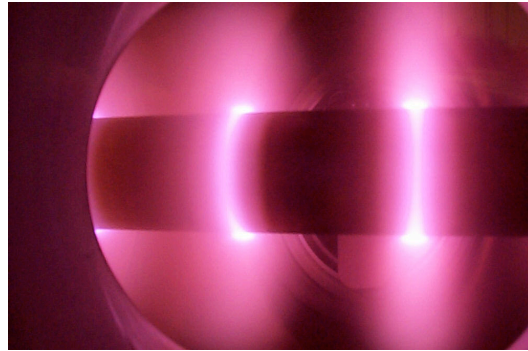


Fig. 4 The discharge plasma during TiN coating of the SNS ring vacuum chambers. The brighter rings are the locations of the spacers between the permanent magnets.

Sample coupons from the coated chambers were analyzed by Auger Electron Spectroscopy (AES). Typical results of AES analysis are shown in Fig. 5. with little oxygen contamination and the correct stoichiometric ratio of Ti and N. The SEY of the coupons were measured by colleagues at CERN in as-received condition, i.e. without *in-situ* bake and with very low accumulative dosage. The coated samples have significantly lower SEY values when compared with bare stainless as shown in Fig. 6.

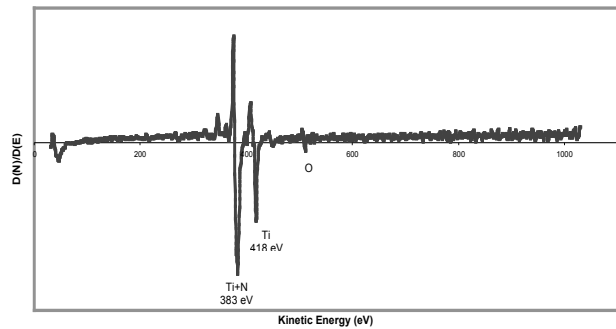


Fig. 5. AES analysis of sputter cleaned TiN sample, showing little oxygen or carbon contamination in the coated film and correct stoichiometric ratio of Ti to N.

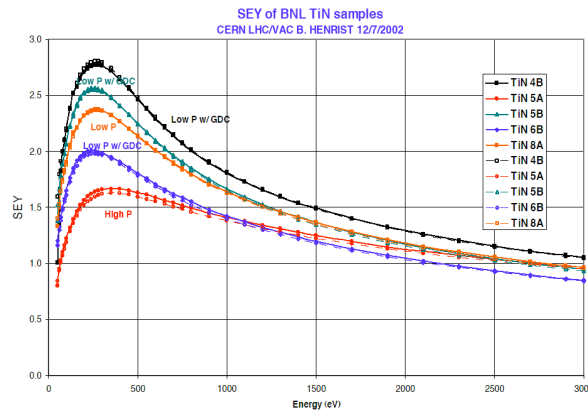


Fig. 6 The SEY value vs. primary electron energy of coated samples at 1.5 mTorr (Low P) and 5 mTorr (high P).

The property of the coated films depends on the sputtering condition. Sputtering at a pressure of  $\sim 5$  mTorr produces a film of brownish color while at 1.5 mTorr, a film of gold color typically associated with that of TiN. Scanning electron microscope (SEM) images reveal that coating of  $\sim 5$  mTorr has a surface with deep voids and grooves, while SEM images of coating of 1.5 mTorr has a smoother surface as shown in Fig. 7. SEY values of the surfaces coated at high and low pressure were measured and found out to differ by a half unit as shown in Fig. 6. The effect of surface roughness on SEY has been reported by Baglin, et-al [7] and is consistent with our study. Thus the SNS TiN coatings are carried out at pressure of  $\sim 5$  mTorr.

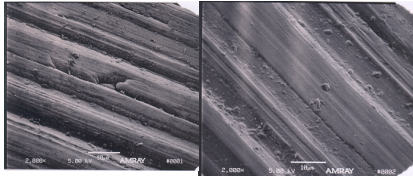


Fig. 7. SEM images of the coated samples, the left-side one was done at pressure of 5 mTorr showing deeper grooves, indicating rougher surface, than the right-side one done at 1.5 mTorr.

In addition to the coating of stainless surfaces, the injection ceramic chambers and the extraction ferrite kickers are also coated with TiN. Ceramic beam pipes are used to minimize Eddy-current heating from the  $\sim 200 \mu\text{s}$  rise time of the injection bumps. The coupling impedance of the ceramic chambers is reduced by an internal conductive coating. They were first coated with  $\sim 0.7 \mu\text{m}$  of copper for beam image current, then  $\sim 0.1 \mu\text{m}$  of TiN to reduce SEY [8]. The resulted Eddy current heating and the disturbance to the kicker field were measured [9] and found to be acceptable.

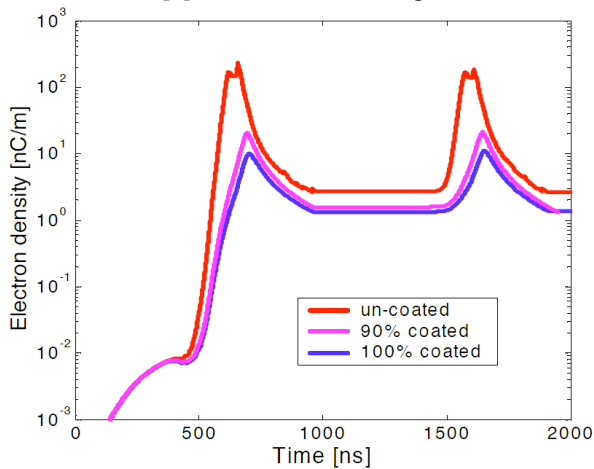


Fig. 8. The electron line density inside the extraction kickers with ferrite surface un-coated, 90% coated and 100% coated, showing a reduction by a factor of ten with TiN coating.

The extraction kicker has rise time in the order of ten nanoseconds. A conductive coating, such as TiN, on the ferrite surface will have a sufficient Eddy current to affect the kicker rise time. Instead, the TiN coating is divided into small strips of 1 cm (vertical) x 5 cm (longitudinal) with 1 mm gaps using custom grid masks which provide a coating on  $\sim 90\%$  of surface while still maintaining a resistance of  $100 \Omega$  or higher between the strips. The estimated disturbance to the kicker rise time is in the order of a nanosecond [10]. The electron line density at the extraction kicker will be a factor of ten lower with 90% of surface covered with TiN as compared with un-coated ferrite surface as shown in Fig. 8.

## SOLENOIDS

Solenoids are wrapped around the beam pipes at the field free regions in the SNS ring, mostly at the collimation and extraction straight sections, where the scattered electrons from beam halo scraping are most prominent. The solenoid field needs to be strong enough so that the radius of the electron motion  $r_\phi = m_e v_e / e B_\phi$  is small compared with the pipe radius ( $r_\phi \sim 10$  mm for a 50 G field for  $E_e \sim 300$  eV where the SEY peaks). The solenoids are fabricated with Kapton insulated gauge 8 copper wire capable of 35 A x 230 turns per meter with an equivalent field of up to 100 G. Simulation and studies have suggested a field of ten gauss will be sufficient to reduce the electron density by a few orders of magnitude [11].

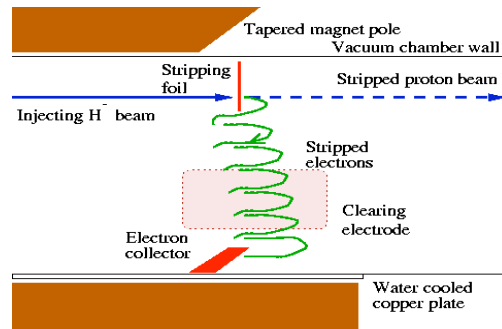


Fig. 9 Schematic layout of the injection area showing the tapered magnet poles to guide the striped electrons from the foil to the carbon-carbon collector, and the dedicated clearing electrode to suppress multipacting.

## ELECTRON CLEARING

Copious electrons are generated at the diamond foil from the  $\text{H}^-$  stripping and the circulating proton scattering. The chicane dipoles are tapered, as shown in Fig. 9, to guide the stripped electrons to an electron collector made of low-Z material (carbon-carbon) and shaped to have a low backscattering yield. A dedicated clearing electrode is implemented inside the stripping-foil assembly. A voltage of up to 10 kV can be applied to this clearing electrode, which is adequate to suppress multipacting in the foil region. There are 44 strip-line type BPMs around the ring as shown in Fig. 10. They may also be used as clearing

electrodes capable of providing a voltage of up to  $\pm 1$  kV, to lower the electron density [11]. To reduce peak electric fields and the resulting electron emission, vacuum ports are screened with rf shields and steps in the vacuum chambers are tapered with a length three times longer than the step height to avoid sharp discontinuities.

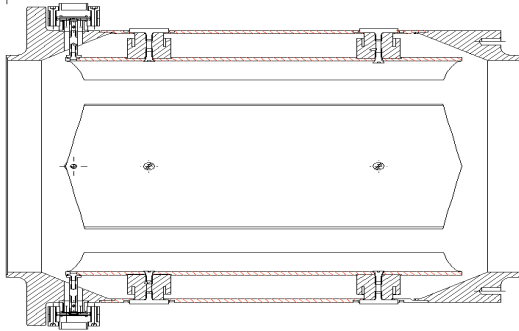


Fig. 10 Strip-line ( $70^\circ \times 4$ ) BPM that can be used as clearing electrodes with voltage up to  $\pm 1$  kV.

### BEAM SCRUBBING

The SEY of the surface can be reduced by scrubbing with energetic electrons [12]. With high intensity in the SNS accumulator ring [1], the electron multipacting will generate a large electron dose on the chamber wall [13]. The pressure will also rise due to the electron stimulated gas desorption, especially at locations having large numbers of primary electrons, such as the injection region and the collimation section. Beam scrubbing is, therefore, proposed as one of the mitigations for the electron multipacting in SNS. It was shown [4] that SEY will be reduced from  $\sim 2.2$  to  $\sim 1.2$  for stainless steel with electron dose of  $\sim 1$  mC/mm<sup>2</sup>. For most machines with electron cloud, the induced beam instability and emittance blowup have prevented high intensity operation, therefore, the benefit of beam scrubbing was not obvious. It is also difficult to use electron dose as a measure of the beam scrubbing due to wide energy range of the electrons. Fortunately, a similar relation exists between the electron dosage and the gas desorption rate. Instead of estimating the electron dose on the chamber wall, the pressure rise has emerged as a more convenient and useful measure of the beam scrubbing effect i.e. if the pressure rise is higher, the beam scrubbing is more effective.

At the design current of  $1.6 \times 10^{14}$  ppp at 60 Hz in SNS ring, the peak electron flux to the wall at the beam tail may reach  $3 \mu\text{A}/\text{mm}^2$  as shown in Fig. 11. The average electron flux will be  $\sim 1$  nA/mm<sup>2</sup>, and the accumulated electron dose  $\sim 0.1$  mC/mm<sup>2</sup> per day. Assuming an electron stimulated gas desorption rate of 0.1, the pressure rise in an average section in SNS ring will be in the order of mid  $10^{-6}$  Torr assuming a linear pumping speed of 30 l/s-m. This pressure level is marginal for the long term operation of the sputter ion pumps. Instead, turbopumps may be reliably used to

maintain the ring pressure during scrubbing or additional sputter ion pumps may be added at the spare pump ports to lower the pressure during scrubbing.

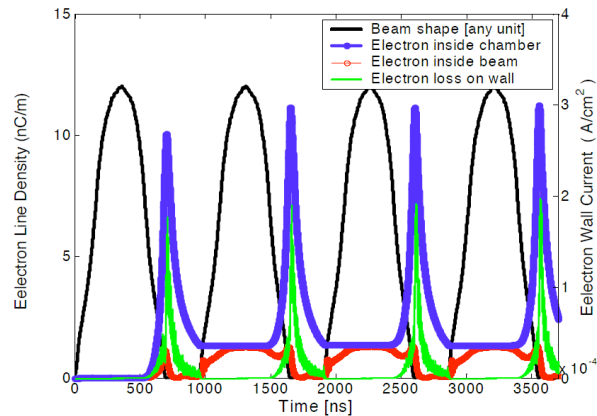


Fig. 11 The electron loss on the wall (green) at the trailing edge of the passing bunches in SNS ring. The peak density is  $\sim 3 \mu\text{A}/\text{mm}^2$ .

### SUMMARY

A number of preventive measures have been implemented in the design and assembly of the SNS ring vacuum systems to suppress the electron generation and improve the electron clearing, which reduce the impact of electron cloud effect. These measures should allow the successful commissioning and operation of SNS up to the designed goal of 1.4 MW beam power without encountering e-p instability and excessive beam loss.

### REFERENCES

- [1] J. Wei, et al, Phys. Rev. ST-AB, **3** (1999) 080101.
- [2] H. Hseuh, et al, Proc. PAC99, p. 1345 (1999).
- [3] J. Wei, et al, Proc. PAC03, p. 2598 (2003).
- [4] N. Hilleret, et al, Proc. PAC99, p. 2629 (1999).
- [5] K. Kennedy, et al, Proc. PAC97, p. 3568 (1998).
- [6] P. He et al, Proc. PAC01, p. 2159 (2001).
- [7] V. Baglin, et-al, Proc. EPAC00, p. 217 (2000).
- [8] P. He, et al, Proc. EPAC02, p. 2556 (2002).
- [9] C. Pai, et al, Proc. PAC03, p. 2144 (2003).
- [10] M. Blaskiewicz, BNL-SNS Tech Note No. 134, April, 2004.
- [11] L.F. Wang, et al, Phys. Rev. ST-AB, **7** (2004) 34401.
- [12] J.M. Jiménez, "Electron Cloud and Vacuum Effect in the SPS", these proceedings.
- [13] L.F. Wang, "Multipacting and Remedies for Electron Cloud in Long Bunch Proton Machine", these proceedings.